Volume 18, Number 5, 2025. pp. 725-736

Jordan Journal of Physics

ARTICLE

Electrospinning of PVA-PEG Blend with Various Cu_2O Nanoparticle Additives: Structural and Dispersion Properties

Akeel S. Alkelaby[a], **Khansaa S. Sharba**[a], **Maher H. Rasheed**[b] and **Khalid H. Abass**[c]

[a] *The General Directorate of Education in Babil, Ministry of Education in Iraq, Iraq.*

[b] *Department of Science, College of Basic Education, University of Babylon, Hilla, Iraq.*

[c] *Physics Department, College of Education for Pure Sciences, University of Babylon, Iraq.*

Doi: **https://doi.org/10.47011/18.5.12**

Received on: 21/02/2025; *Accepted on: 17/07/2025*

Abstract: This project entailed the synthesis of novel nanofibers by the electrospinning technique. The nanofibers included Poly (vinyl alcohol) (PVA) and polyethylene glycol (PEG) doped with different concentrations (0.002, 0.004, 0.006) of copper oxide (Cu_2O) at room temperature. Images from the optical microscope (OM) revealed a fine and homogenous dispersion of the nanomaterials. This was corroborated by Scanning Electron Microscopy (SEM) analysis, which showed that the delicate fibers in both the polymer blend and doped samples were randomly distributed and no signs of nanoparticle aggregation were detected. Prior to the incorporation of the Cu_2O additive, the nanofibers demonstrated an average diameter of 68.97 nm, while the inclusion of Cu_2O at varying concentrations yielded average diameters of 64.14 nm for 0.002 g, 71.35 nm for 0.004 g, and 68.46 nm for 0.006 g. Notably, these nanofibers maintained a smooth surface morphology across all samples. The transmittance progressively decreases, starting at a value of 0.996 for the unmodified PVA-PEG blend and reducing to 0.978 as the Cu_2O concentration reaches 0.006. Concurrently, the extinction coefficient demonstrates increase, rising from 0.001027 to 0.00475 with higher Cu_2O content. Similarly, the real part of the dielectric constant increases from 1.4559 to 2.1044, while its imaginary part expands from 0.00247 to 0.0137. The Wemple-DiDomenico model was utilized to compute the dispersion coefficients, comprising E_o, E_d, n_o, M_{-1}, and M_{-3}.

Keywords: PVA-PEG-Cu_2O, Nanofiber, Electrospinning, SEM, Dispersion parameters.

Introduction

Polymers have rapidly become an indispensable component of modern life, owing to their versatility, affordability, low operational expenses, ease of processing, and desirable chemical, physical, and optical properties [1]. A polymer is comprised of countless molecules, each including thousands atoms held together with covalent bonds. In addition, the molecules in a polymer are attracted to each other by various forces depending on the type of polymer [2]. Like conventional composites, a nanocomposite is made of a matrix and filler. But nanocomposites use nanoparticle fillers instead of fiber fillers used in conventional composites such as carbon or fiberglass [3]. Examples of the former include CNTs, carbon nanofibers, and other semiconductor or metal nanoparticles such as silicon, gold, silver, diamond, and copper [4]. Polymer nanofibers are an important category of nanostructured materials, with potential uses in numerous fields such as biology, electronics, medicine, protective gear, and water treatment. Recent advancements in preparation techniques such as phase separation, electrospinning, drawing, and template synthesis have enabled improvement in

Corresponding Author: Khalid Haneen Abass **Email**: pure.khalid.haneen@uobabylon.edu.iq

production processes and expanded the range of possible applications [5]. Electrospinning technique is particularly renowned for its simplicity, low expense, flexibility, and ability to manufacture one-dimensional nanostructured materials. Among all the various techniques one can use for producing such materials inexpensively and with versatility, electrospinning is particularly worth mentioning [6].

PVA or polyvinyl alcohol is increasingly being known as a highly promising polymer with some mind-boggling properties. They are characterized by good water solubility, good dielectric strength, chemical stability, and environmental friendliness. The hydroxyl groups in PVA facilitate the formation of strong interlinks in polymer composites through hydrogen bonding [7]. Poly vinyl alcohol, or PVA, is commonly used in various industries such as electronics, construction, medicine, and others. The reason is that the polymer has numerous advantages such as its water solubility and exceptional flexibility, which make it highly versatile and effortless to apply across a wide range of industrial purposes. Additionally, it is regarded as safe for both medical and food-related applications [8].

Polyethylene glycol, or PEG, is a common polymer that is widely in demand due to its availability, low cost, and safety [9]. Polyethylene glycols, or PEGs, are a family of polymers containing a variety of properties which may be liquid or solid [10]. To enhance the elasticity, additional polymers can be incorporated for the same. Utilization of plasticizers relaxes the molecular rigidity by decreasing the intermolecular forces along the polymer chain [11].

Cuprous Oxide (Cu_2O) has come into new focus for several technological applications based on its optoelectronic properties [12, 13]. The Pn3m is the space group of Cu_2O with the unit cell consisting of two copper, and four oxygen ions. These are placed with oxygen atoms in a body center cubic enclosed lattice with tetrahedrally surrounding copper ions [14]. The Cu_2O is considered an excellent photovoltaic material due to the abundance of copper on Earth, its high theoretical energy conversion efficiency of approximately 20%, its non-toxic nature, and its cost-effective production. The other reason for using Cu2O as an absorber is due to its high absorption coefficient in the visible region and its direct bandgap nature of 2.1 eV [15-17]. In recent years, Cu_2O has attracted considerable attention because of its promising applications in lithium-ion batteries [18], nanomagnetic devices [19], photocatalysis [20], transistors [21], gas sensors 22] photodetector [23] and solar cell 24,25]. In this study, we report the electrospinning fabrication of PVA-PEG-Cu2O nanofibers, and investigate their optical properties and dispersion parameters for application as a promising candidate for communication and optical devices.

Experimental

Preparation of PVA-PEG/ Cu_2O Nanofibers

In order to synthesize 2 g of PVA-PEG polymer nanofibers, the process was initiated by dissolving 1.6 g of PVA powder in 60 mL distilled water using a glass flask with a magnetic stirrer. After 45 minutes of stirring at 90 °C, the solution was completely homogenized. To this 0.4 gram of PEG was added dropwise at 90 °C.The blending was continued for a further 45 minutes until a hick homogeneous solution formed. The stirring of suspension was continued during the process to increase homogeneity. Afterwards, three portions of Cu2O (0.002; 0.004 and 0.006 g) were added into the solution while, every portion was sonicated for two minutes to disperse it throughout the mixture. After each addition of Cu2O, the mixture was left stirring for 45 min for good dispersion. As shown in Table 1, the resultant mixture was then utilized for electrospinning to produce (PVA-PEG) nanofibers with varied degrees of Cu_2O additions.

TABLE 1. Weight of PVA-PEG- Cu_2O nanocomposites.

PVA (g)	PEG (g)	Cu_2O (g)
1.6	0.4	0.0
1.6	0.4	0.002
1.6	0.4	0.004
1.6	0.4	0.006

Electrospinning Process

The solution was inserted into a 2 mL syringe that was outfitted with a stainless-steel needle after it had been thoroughly mixed. The hypodermic was subsequently positioned in front of a metal collector that was horizontally oriented. During the electrospinning process, the needle tip served as the positive electrode, while the metal collector served as the negative electrode. To make material deposition easier, the collector was covered with aluminum foil. The spinning parameters are specified in Table 2, and the electrospinning was performed at room temperature.

TABLE 2. Electrospinning Parameters for Specimen Fabrication.

Electrospinning parameters	Specification
applied voltage	24 KV
Collector distance	10 cm
Orifice size	0.7 mm
rotation speed	500 rpm
temperature	25 °C
flow rate	0.5 ml/hr

Results and Discussion

Fig.1, Table 1 shows SEM micrographs of PVA-PEG polymer blend and Cu_2O embedded in the PVA-PEG composite at concentration of 0.002, 0.004 and 0.006 magnification at x20kV and x110Kv respectively. These pictures corroborate the analysis of surface topology of the samples and distribution of Cu_2O in polymer matrix.

The average fiber diameter was 68.97 nm before use of Cu_2O. The fiber diameters were between 64.14 and 68.46 nm after the Cu2O loading determined by ImageJ software. The nanofibers had a smooth surface, while the microfibers were irregularly distributed as well as having crossing points. The stability of the liquid filament in the process of electrospinning depends mainly on molecular entanglement [26] that is an important factor for fibre structuring and homogeneity in this technique. During electrospinning, changes in fiber morphology and/or bead formation can occur as a result of interactions between solution characteristics and experimental conditions. The structure differences may be affected by the polymer-related parameters such as molecular weight, polydispersity index, glass transition temperature (Tg), isomeric structures and cross-linking.

These might also be associated with the solution (eg, composition of solvent, concentration, viscosity, electrical conductivity and dielectric strength as well as surface tension of the liquid), process (like magnitude of applied field strength, distance for deposition etc.), 42 - 44 like flow rate or electric current passed through an instrument or deposition time) or postdeposition treatment. [27]. The influence of various parameters on the morphology of electrospun polymers is illustrated in Fig. 2 [28]. Among the various electrospinning parameters, the concentration of the polymer solution plays a crucial role in fiber generation. The solution is characterized by reduced viscosity and increased surface tension when the concentration is insufficient, which leads to the formation of polymeric micro- or nanoparticles through electrospray rather than fiber development [29]. Conversely, a minor increase in concentration results in a blend of fibers and pearls. But the production of silky and homogenous nanofibers is successful if the concentration is at an optimal level [30]. Electrospun fiber morphology is also significantly influenced by viscosity. Continuous and uniform filaments are significantly opposed by low viscosity, and high viscosity can oppose the expulsion of the liquid projectile out of the solution. Proper viscosity should thus be achieved for the successful completion of electrospinning [31, 32].

Also, surface tension, which is dominated by the solvent component in large part, is one of the critical parameters for electrospinning [33]. It is well known that the shear viscosity of the mixture determines the typical diameter of nanofibers produced by electrospinning. As viscosity increases, nanofibers of greater diameters will tend to be formed, as in Eq. (1) [34]. Briefly, the diameter and morphology of nanofibers generated through electrospinning are significantly influenced by the polymer solution's viscosity and concentration and surface tension. To achieve the desired fiber properties in electrospinning, one has to achieve

an appropriate balance between these parameters.

$$d \sim \eta^{\lambda} \quad (1)$$

The given Eq. (1) establishes the connection between the average electro spun fiber diameter (d), the solution's shear viscosity (η), and the yielding exponent (λ). The exact value of the yielding exponent (λ) differs based on the particular polymer solution used, however it is usually more than 1/3 as per the scaling equation [35].

Both the voltage and viscosity of the polymer solution should be maintained within a range that is optimal for efficient electrospinning. Some factors like polymer concentration, solution flow rate, working distance, and applied voltage in the electrospinning device all together control the production of uniform morphology continuous fibers with minimal bead formation. However, extremely high solution concentration has a negative influence on the production of nanofibers as improper levels of viscosity may hinder fiber formation [36].

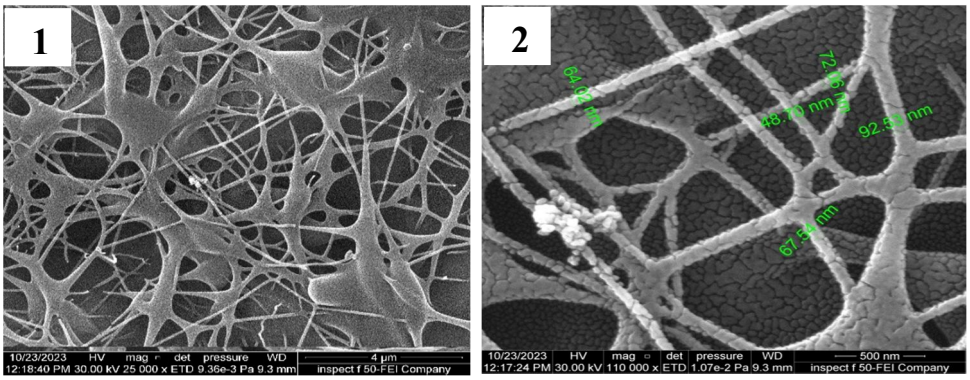

FIG. 1(A). The scanning microscopy pictures of PVA-PEG nanofibers taken at two different magnifications, 25 kx and 110 kx.

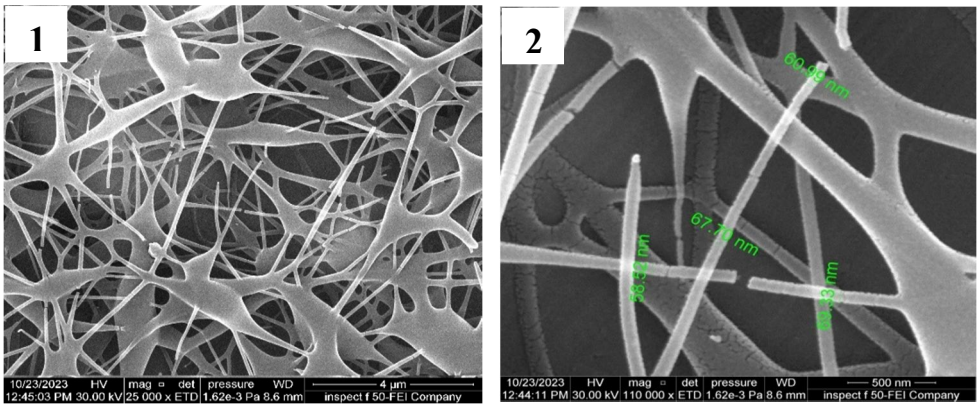

FIG. 1(B). Scanning electron micrographs taken at two different magnifications, 25 kx and 110 kx, of electrically spun PVA-PEG nanofibers containing 0.002 g Cu_2O.

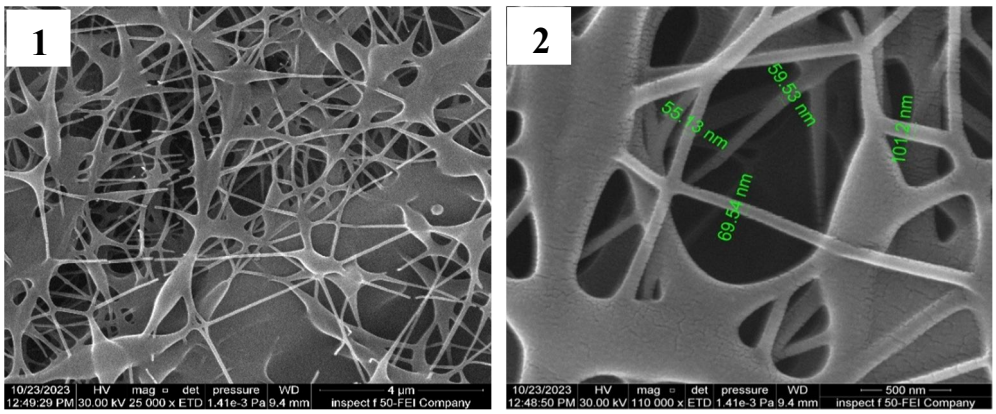

FIG. 1(C). Scanning electron micrographs taken at two different magnifications, 25kx and 110 kx, of electrospun PVA-PEG nanofibers containing 0.004 g Cu_2O.

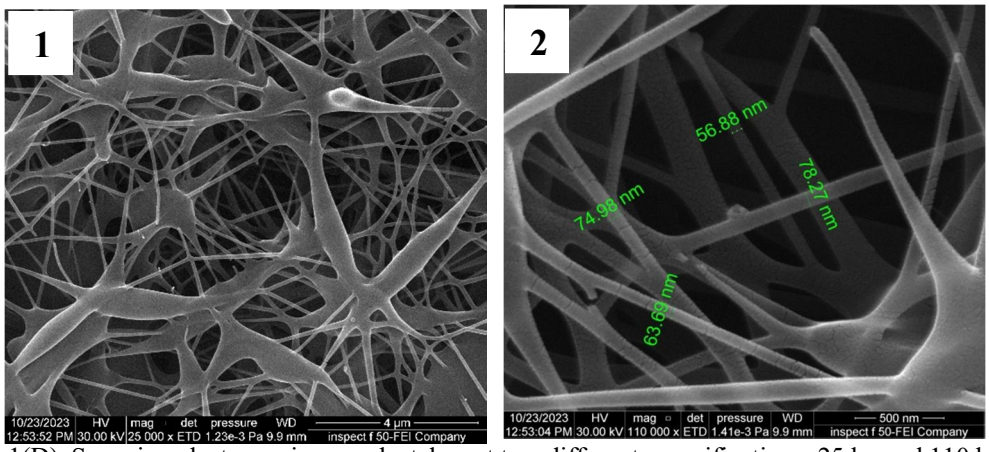

FIG. 1(D). Scanning electron micrographs taken at two different magnifications, 25 kx and 110 kx, of electrically spun PVA-PEG nanofibers containing 0.006 g Cu_2O.

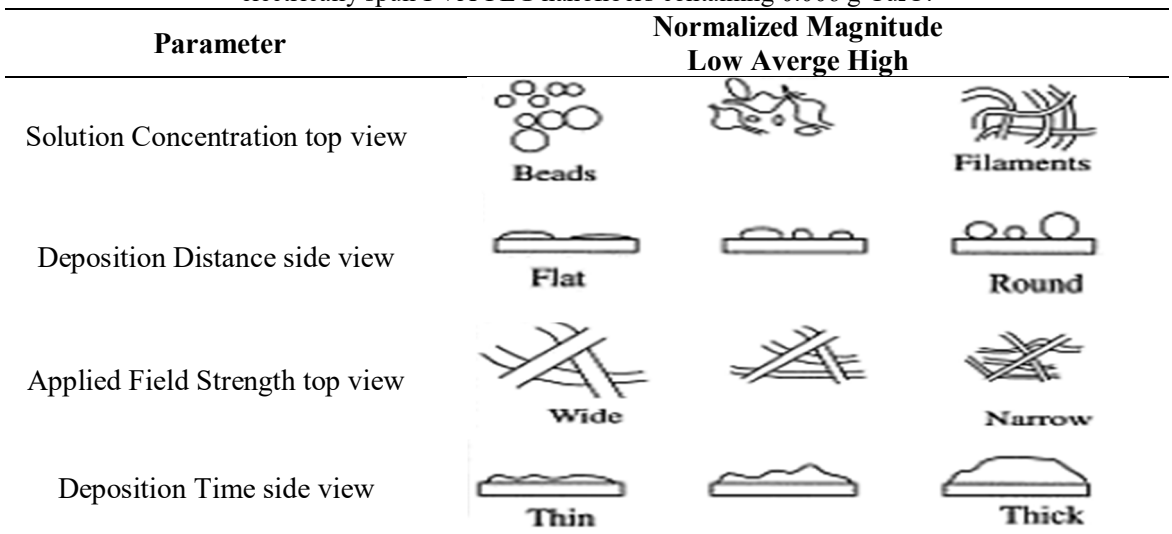

FIG. 2. a schematic representation of the impact of process parameters on the electro spun product's structure.

The optical microscope (OM) images verify the successful fabrication of PVA-PEG- Cu_2O nanofibers using the casting method. These images expose a uniform matrix with Cu_2O evenly distributed throughout the polymer blend composites. In particular, Fig. 3(a) displays the PVA-PEG blend, signifying the effective dissolution of the polymers. Parts (b, c, and d) of Fig. 3 illustrate the diffusion of Cu_2O within the PVA-PEG blend, revealing a well-dispersed distribution of nanoparticles within the blend.

Importantly, there is no nanoparticle aggregation observed to be due to the interaction between polymers and Cu2O as a result of high surface area volume ratio. At a Cu2O nanofiber weight, or loading, of 0.006 a network of pathways are established for charge carriers to transport via. This results in alteration of the material characteristics [37].

The transmittance spectra (T) were calculated by [38]:

$$T = I_T/I_o \quad (2)$$

where I_T is the intensity of transmitted rays from the film and I_o intensity of incident rays on the film.

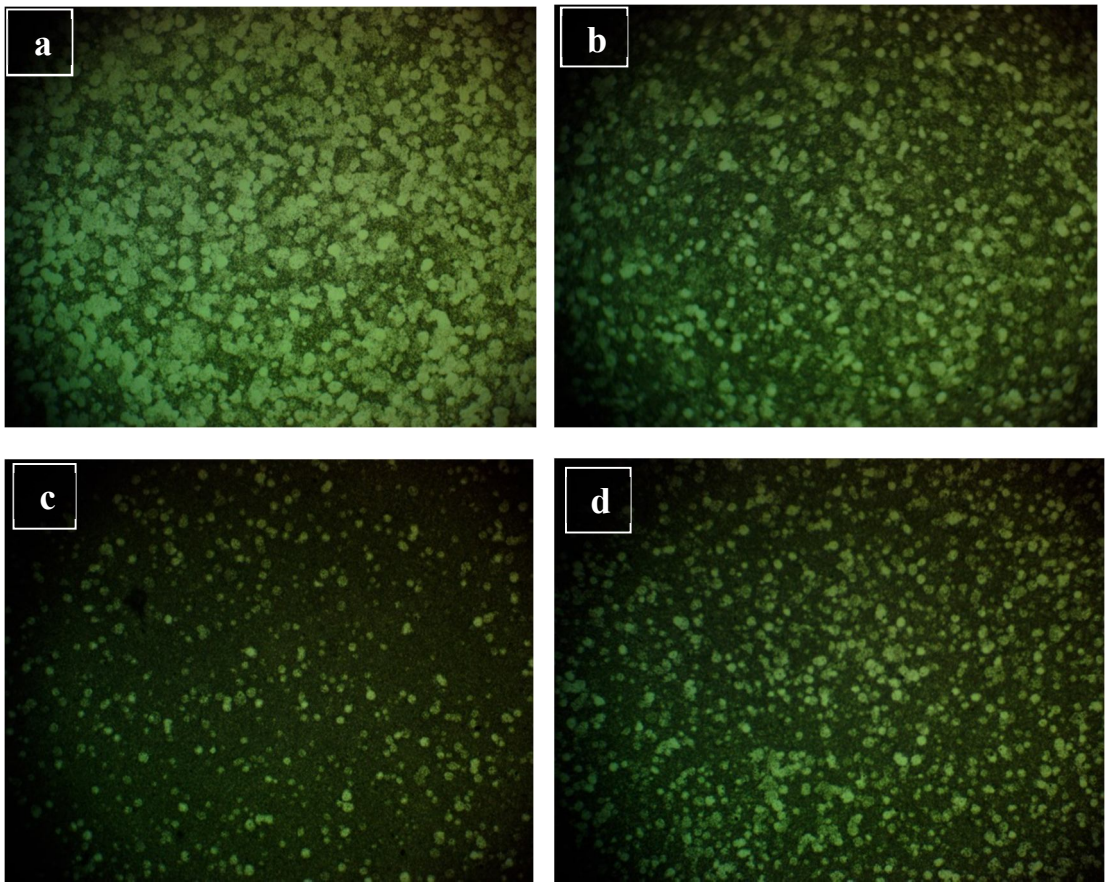

FIG. 3. Photomicrographs (100X) of (PVA- PEG) with add various content of Cu_2O: (A) 0 Cu_2O (B) 0.001 Cu_2O (C) 0.002 Cu_2O and (D) 0.003 Cu_2O.

Figure 4 presents the transmittance (T) spectra of PVA-PEG-Cu_2O nanofibers with varying concentrations of Cu_2O as a function of wavelength. Unlike the absorption spectra, the transmittance decreases progressively, starting from 0.996 for the pure PVA-PEG blend and lowering to 0.978 as the Cu_2O concentration increases up to 0.006. This observed reduction in transmittance is attributed to the incorporation of Cu_2O, which contains electrons capable of absorbing electromagnetic energy and transitioning to higher energy states. In contrast, the pure PVA-PEG sample shows significantly high transmittance due to the absence of particles. Without free electrons, such a sample requires much higher energy for electronic transitions or bond disruption [39].

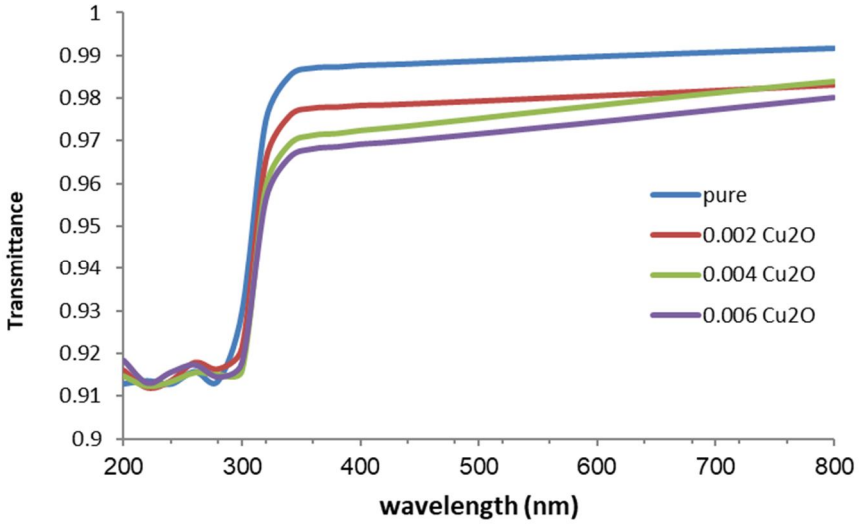

FIG. 4. The transmittance versus wavelength of PVA-PEG blend and PVA-PEG-Cu_2O Nanocomposites.

The extinction coefficient (k_o) was calculated by [40]:

$$k_o = \alpha\lambda/4\pi \quad (3)$$

Figure 5 shows the extinction coefficient (k_o) for PVA-PEG- Cu_2O nanofibers across a range of wavelengths. It shows a marked increase with higher concentrations of Cu_2O. This trend can be ascribed to the enhanced optical absorption and photon dispersion within the as the concentration of Cu_2O increases, the PVA-PEG polymer composite increases. The nanofiber samples' substantial absorbance within this range is the primary reason for the extinction coefficient's elevated values in the UV region. As a result, the nanofibers' extinction coefficient is notably pronounced at UV wavelengths. Although the absorption coefficient of the nanofibers remains relatively consistent from the visible to the near-infrared spectrum, the extinction coefficient exhibits an upward trend as the wavelength increases [41].

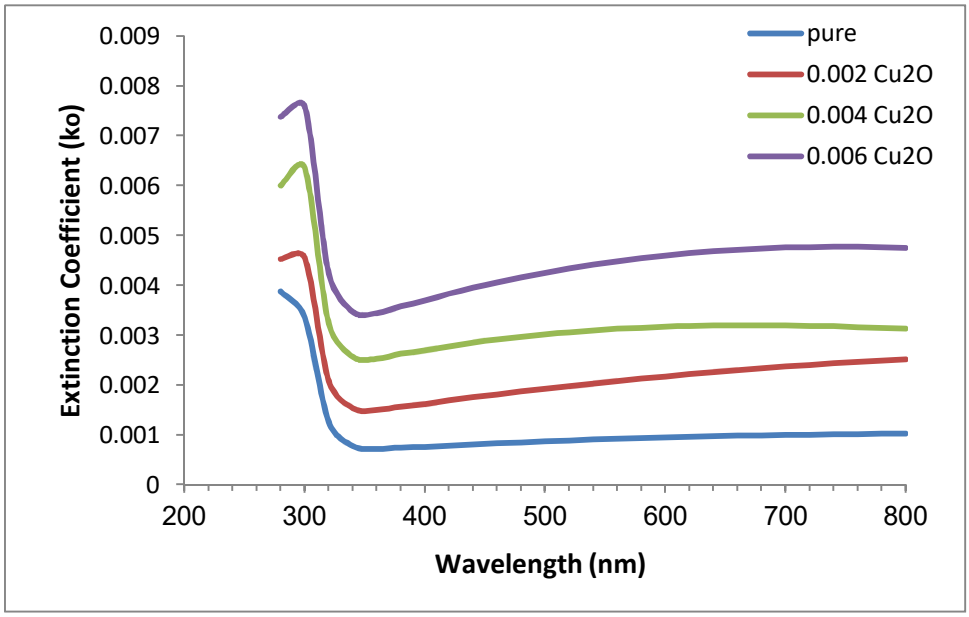

FIG. 5. The extinction coefficient versus wavelength of PVA-PEG blend and PVA-PEG -Cu_2O Nanocomposites.

Dielectric constants for two parts real (ε_1) and imaginary (ε_2) were calculated by [42]:

$$\varepsilon_1 = n^2 - k_0^2 \quad (4)$$

$$\varepsilon_2 = 2n\,k_0 \quad (5)$$

The dielectric constant is the basic source of information about the electronic band structure of materials. Slowing down light in a material is associated with the real part of the dielectric constant (ε_1), while the imaginary part (ε_2) is a key optical parameter linked to both the refractive index and the extinction coefficient.

Figures 6 and 7 show the variation of real and imaginary parts of the dielectric constant for PVA-PEG-Cu_2O nanofibers with wavelength and Cu_2O concentration.

It can be seen that both parts of the dielectric constant increase with the rise in Cu_2O concentration. This is because there is increased electrical polarization in the nanofibers, which results from the higher concentration of Cu_2O in the sample. This results in the increase in charges in the polymers that make up both the PVA-PEG blends and the PVA-PEG-Cu_2O nanofibers proportionally. The two figures also show the changes in real and imaginary part of dielectric constant versus wavelengths. This behavior is primarily due to ε1 depending more on the refractive index, and less on the extinction coefficient. In contrast, the absorbance value of the imaginary part (ε2) is significantly influenced by an increased extinction coefficient depending on wavelength and less by a refractive index that remains relatively constant, particularly in the visible and near-infrared regions. [43, 44].

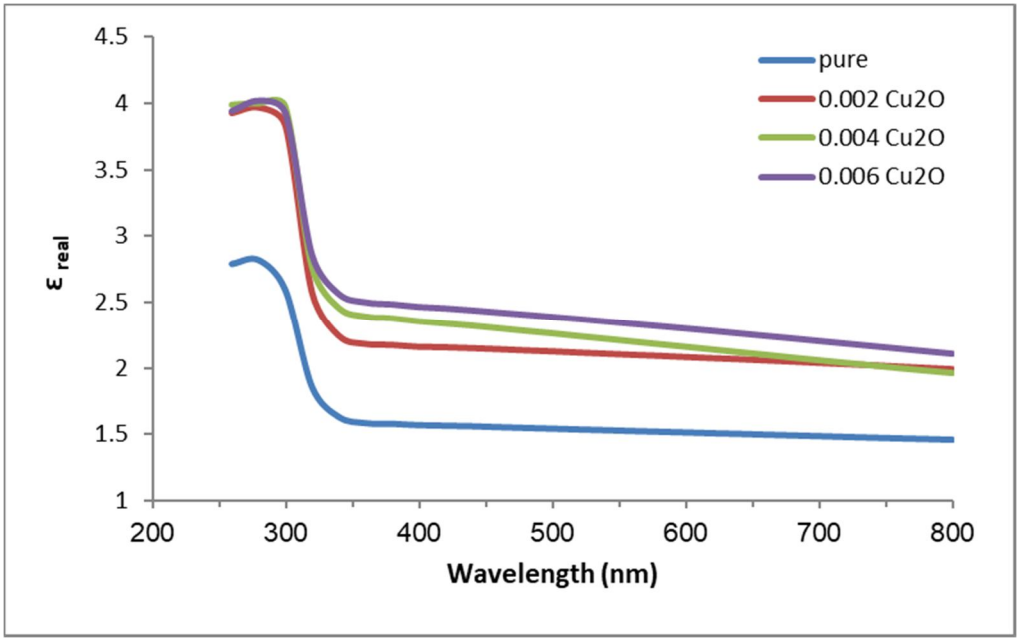

FIG. 6. The real dielectric constant with the wavelength of PVA-PEG blend and PVA- PEG-Cu_2O nanocomposites.

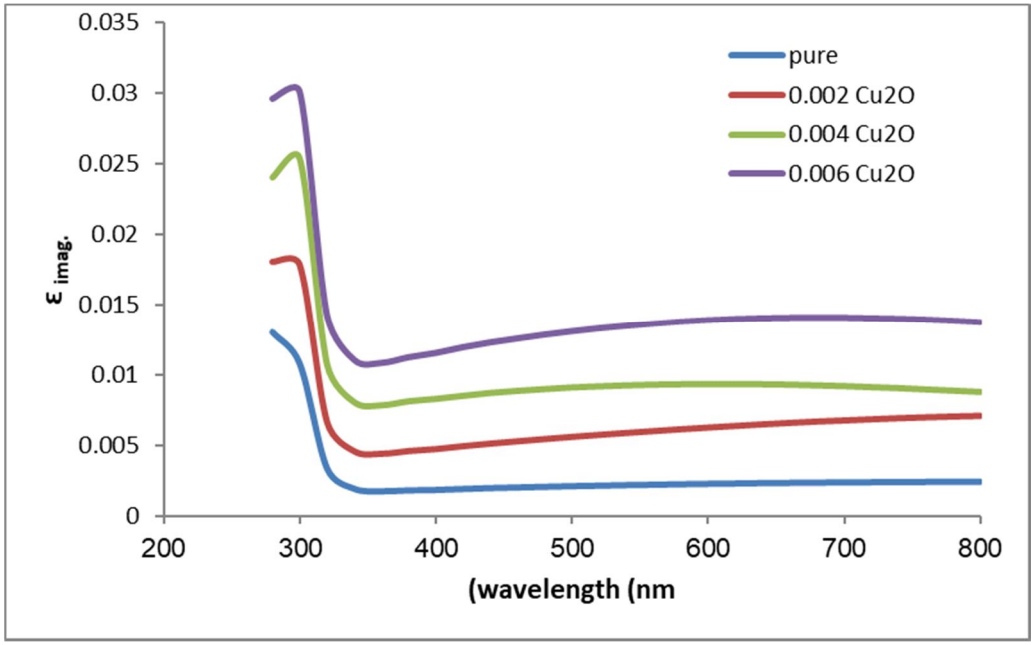

FIG. 7. The imaginary dielectric constant with the wavelength of PVA- PEG blend and PVA- PEG -Cu_2O nanocomposites.

Dispersion Parameters

The refractive index dispersion of materials has been analyzed using the single-oscillator model, which introduces the energy parameters E_d (dispersion energy) and E_o (oscillator energy). According to the Wemple and DiDomenico model, the refractive index (n) at a given photon energy *(hv)* can be expressed for both PVA-PEG blend and PVA-PEG-Cu_2O nanofibers. From the equations (6-10) the values E_o, E_d, E_g, n_0, ε_∞, M_{-1} and M_{-3} were calculated [45-49].

$$(n^2 - 1) = \frac{E_d E_o}{{E_o}^2 - (h\upsilon)^2} \quad (6)$$

$$n_0^2 = 1 + \frac{E_d}{E_o} \quad (7)$$

$$\varepsilon_\infty = n_0^2 \quad (8)$$

$$E_o^2 = \frac{M_{-1}}{M_{-3}} \quad (9)$$

$$E_d^2 = \frac{M_{-1}^3}{M_{-3}} \quad (10)$$

From the graphic representation of the relationship between $(n^2 - 1)^{-1}$ and $(h\upsilon)^2$ in

Fig. 8 used the slope $(E_0\ E_d)^{-1}$ and the intercept $(\frac{E_0}{E_d})$ to determine E_0 and E_d. Table 3 contained the calculated value, which demonstrated a decline in their values when (Cu_2O)NPs concentrations increased, the oscillator strength (E_o) and the dispersion energy linked with the energy of optical transitions (E_d) are shown to decrease as (Cu_2O)NPs increases, but the other parameters n_0, ε_∞ $M_{-1}$and M_{-3} increase. This phenomenon can be attributed to the shift of the optical transmission spectra toward longer wavelengths, which corresponds to the absorption edge shifting toward lower energy wavelengths and rise in nanomaterials' concentration results in a reduction in interparticle spacing, thereby intensifying interparticle interactions, which leads to a decrease in dispersion-related parameters. Additionally, elevated concentrations of nanomaterials significantly influence the material's optical characteristics, further contributing to variations in the dispersion parameters. The calculated optical energy gap (the approximation relation $E_o \approx 2E_g$) using the Tauc relation and the Wemple-DiDomenico estimate both had similar values. The findings concur with those of earlier researchers [50].

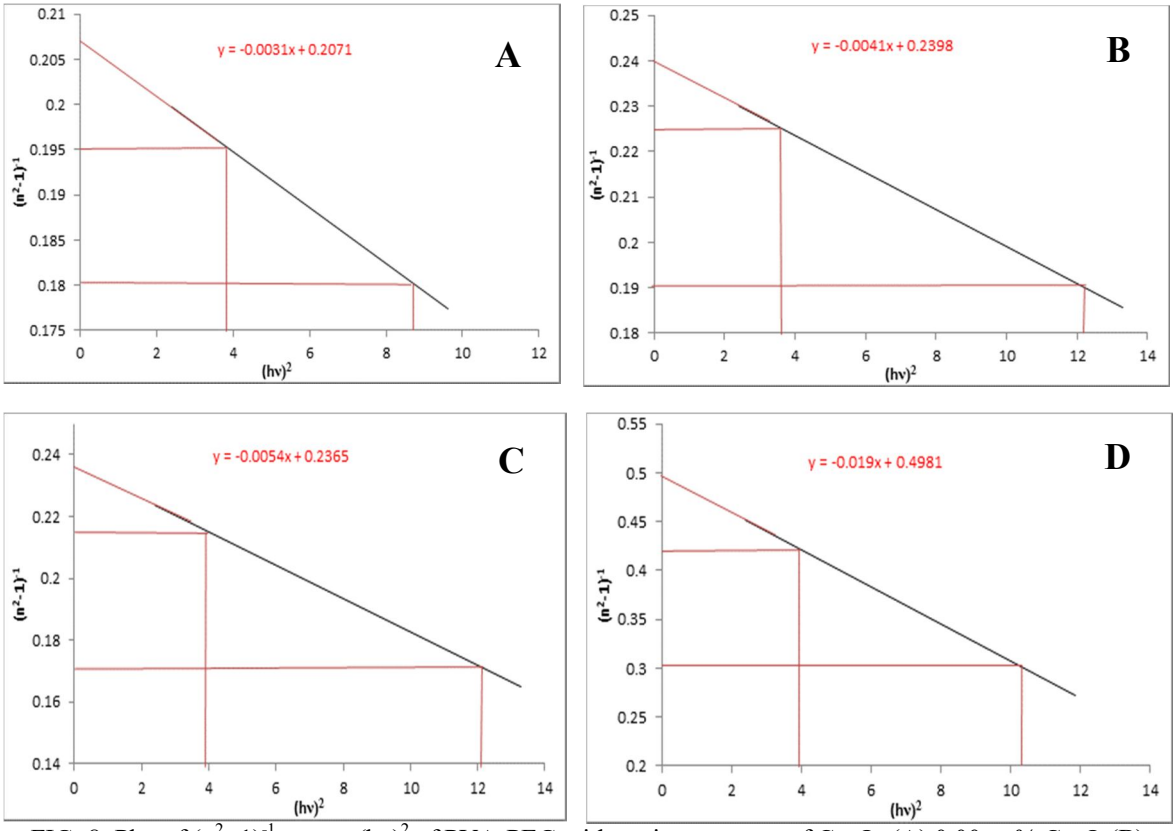

FIG. 8. Plot of $(n^2 -1)^{-1}$ versus $(h\upsilon)^2$ of PVA-PEG with various content of Cu_2O: (A) 0.00wt.% Cu_2O (B) 0.002wt.% Cu_2O (C) 0.004wt.% Cu_2O and (D) 0.006wt.% Cu_2O.

TABLE 3. Optical parameters of PVA-PEG -Cu_2O nanofibers.

parameter	0 wt.	0.002wt. Cu_2O	0.004wt. Cu_2O	0.006wt. Cu_2O
E_o	67.62	57.600	42.426	26.541
E_o	8.223	7.589	6.513	5.151
slope	0.003	0.004	0.005	0.018
E_g	4.111	3.794	3.256	2.575
E_d	39.725	31.622	27.367	10.514
n(0)	5.830	5.166	5.201	3.040
$n_o(0)$	2.414	2.273	2.280	1.743
ε	5.830	5.166	5.201	3.040
M_{-1}	4.830	4.166	4.201	2.040
M_{-3}	0.071	0.0723	0.099	0.076

Conclusion

Nanofibers of PVA-PEG-Cu_2O were synthesized with success by refining the electrospinning parameters, which included the careful adjustment of the spinning solution composition, applied voltage, spinning distance, and flow rate. Before incorporating Cu_2O, the nanofibers had an average diameter of 68.97 nm. The integration of Cu_2O resulted in average diameters ranging from 64.14 nm to 68.46 nm. Scanning electron microscopy analyses validated the presence of a smooth surface morphology in these fibers, while optical microscopy images revealed a homogenous distribution of the nanomaterial throughout the samples. The transmittance exhibited a gradual decrease, beginning at 0.996 for the pur PVA-PEG blend, and declining to 0.978 when the Cu_2O concentration increased to 0.006. Additionally, the extinction coefficient displayed a rising trend, increasing from 0.001027 to 0.00475 with higher Cu_2O content. The real part of the dielectric constant increased from 1.4559 to 2.1044, and the imaginary part grew from 0.00247 to 0.0137 as the concentration of Cu_2O augmented. Moreover, dispersion parameters, such as E_o, E_d, n_o, M_{-1}, and M_{-3}, were calculated utilizing the Wemple-DiDomenico model. These findings concerning dispersion parameters are instrumental in advancing the design and fabrication of optical devices.

Author Contribution Statement

Akeel Shakir Alkelaby, Khansaa Saleem Sharba, Maher Hassan Rasheed, and Khalid Haneen Abass contributed equally to this work. Akeel Shakir Alkelaby and Khansaa Saleem Sharba were primarily responsible for the study's conceptualization, design, methodology development, and data analysis. Maher Hassan Rasheed and Khalid Haneen Abass focused on the experimental work, data collection, and initial manuscript drafting. All authors participated in the review and editing process, provided critical revisions, and approved the final version.

Funding

This research received no specific grant from any funding agency in the public, commercial, or not-for-profit sectors.

Data Availability Statement

I have read and accept the terms of the Share Upon Reasonable Request data policy.

Statements and Declarations

This paper reports on a detailed study of the electrospinning of PVA-PEG blend matrices which contain Cu_2O nanoparticles in various additives with an emphasis on their structure and dispersion behaviour.

Competing interests

The authors have declared that no competing interests exist.

Acknowledgement

The authors are thankful to the staff at Babylon University for their cooperation and support.

References

[1] Radwan, R.M., J. Phys. D. Appl. Phys., 40 (2) (2007) 374.

[2] Al Asadi, S.M., Hamood, F.J., Abass, K.H., Mohammed, S.K., Hassan, I.M., and Latif, D.M.A., Research Journal of Pharmacy and Technology, 12 (6) (2019) 2768.

[3] Robertson, J., Materials Today, 7 (2004) 46.

[4] Devangamath, S.S. et al., J. Mater. Sci. Mater. Electron., 31 (2020) 2904.

[5] Beachley, V. and Wen, X., Prog. Polym. Sci., 35 (2010) 868.

[6] Shenoy, K.A., M.Sc. Thesis, Department of Mechanical Engineering, Wichita State University (2008).

[7] Ben Doudou, B., Vivet, A., Chen, J., Laachachi, A., Falher, T., and Poilâne, C., J. Polym. Res., 21 (4) (2014) 1.

[8] Abdali, K., Al-Bermany, E., and Abass, K.H., J. Polym. Res., 30 (4) (2023) 138.

[9] Abu-Zied, B.M. and Asiri, M.A., Int. J. Electrochem. Sci., 10 (6) (2015) 4873.

[10] Chieng, B.W., Ibrahim, N.A., Yunus, W.M.Z.W., and Hussein, M.Z., Polymers, 6 (2014) 93.

[11] Abass, K.H. and Hamed, A., J. Green Eng., 10 (7) (2020) 4166.

[12] Sawant, S.S., Bhagwat, A.D., and Mahajan, C.M., J. Nano-Electron. Phys., 8 (1) (2016) 01035(1-5).

[13] Jayathilaka, C., Kumara, L.S.R., Ohara, K., Song, C., Kohara, S., Sakata, O., Siripala, W., and Jayanetti, S., Crystals, 10 (2020) 609.

[14] Isah, K.U., Bakeko, M., Ahmadu, U., Uno, U.E., Kimpa, M.I., and Yabagi, J.A., IOSR J. Appl. Phys., 3 (2) (2013) 61.

[15] Gevorkyan, V.A., Reymers, A.E., Nersesyan, M.N., and Arzakantsyan, M.A., Int. Symp. Optics and Its Applications (OPTICS2011), 350 (2012) 012027.

[16] Umar, M., Swinkels, M.Y., De Luca, M., Fasolato, C., Moser, L., Gadea, G., Marot, L., Glatzel, T., and Zardo, I., Thin Solid Films, 732 (2021) 138763.

[17] Abbas, A. and Abass, K.H., Mater. Today: Proc., 60 (2022) 1402.

[18] Wei, H.M., Gong, H.B., Chen, L., Zi, M., and Cao, B.Q., J. Phys. Chem. C, 116 (19) (2012) 10510.

[19] Bai, Y., Yang, T., Gu, Q., Cheng, G., and Zheng, R., Powder Technol., 227 (2012) 35.

[20] Tuama, A.N., Abass, K.H., and Bin Agam, M.A., Int. J. Nanoelectron. Mater., 13 (3) (2020) 601.

[21] Salek, G., Tenailleau, C., Dufour, P., and Guillemet-Fritsch, S., Thin Solid Films, 589 (2015) 872.

[22] Lupan, O. et al., Sens. Actuators B Chem., 224 (2016) 434.

[23] Lee, W-J. and Wang, X-J., Coatings, 11 (2021) 864.

[24] Siol, S. et al., ACS Appl. Mater. Interfaces, 8 (33) (2016) 21824.

[25] Alkelaby, A.S. et al., J. Glob. Pharma Technol., 11 (4) (2019) 347.

[26] Talafha, M.F., Shaltoutb A.M.K., Abdelkawy A.G.A., and Behearyn M. Jordan Journal of Physics,18 (4) (2025) 551.

[27] Jose, J., Al-Harthi, M.A., AlMa'adeed, M.A.A., Dakua, J.B., and De, S.K., J. Appl. Polym. Sci., 132 (16) (2015).

[28] Mousa, M.S. and Hagmann, M.J. Jordan Journal of Physics, 18(4) (2025) 455.

Schubert, D.W., Macromol. Theory Simul., 28 (2019) 1900006.

[29] Wang, Q. et al., Anal. Chim., 2018 (2018) 125.

[30] Jia, Y.T., Gong, J., Gu, X.H., Kim, H.Y., Dong, J., and Shen, X.Y., Carbohydr. Polym., 67 (2007) 403.

[31] Rasheed, M.H., Hashim, F.S., and Abass, K.H., Int. J. Nanosci., 22 (3) (2023).

[32] Qader, K.Y., Ghazi, R.A., Jabbar, A.M., Abass, K.H., and Chiad, S.S., J. Green Eng., 10 (10) (2020) 7387.

[33] Zhang, M., Liu, Y.J., Xu, T.Y., and Sun, D.H., Adv Material Res, 332 (2011).

[34] Sharba, K.S., Alkelaby, A.S., and Abass, K.H., Plasmonics, 20 (2025) 6807.

[35] Mohammed, H.R.A., Al-Ogaili, A.O.M., and Abass, K.H., Mater. Today: Proc., 80 (2023) 2396.

[36] Alkelaby, A.S., Ahmadi, M.T., Esmaeili, A., Sedghi, H., and Abass, K.H., Polym. Bull., 81 (2024) 17377.

[37] Sakhil, M.D., Shaban, Z.M., Sharba, K.S., Habubi, N.F., Abass, K.H., Chiad, S.S., and Alkelaby, A.S., NeuroQuantology, 18 (5) (2020) 56.

[38] Chiad, S.S., Alkelaby, A.S., and Sharba, K.S., J. Glob. Pharma Technol., 11 (7) (2019) 662.

[39] Da Silva, M.A., Crawford, A., Mundy, J., Martins, A., Araújo, J.V., Hatton, P.V., Reis, R.L., and Neves, N.M., Tissue Eng. Part A, 15 (2) (2009) 377.

[40] Abass, K.H. and Obaid, N.H., J. Phys. Conf. Ser., 1294 (2) (2019).

[41] Tuama, A.N., Abass, K.H., and Bin Agam, M.A., Optik, 247 (2021) 167980.

[42] Sharba, K.S., Alkelaby, A.S., and Abass, K.H., Revue des Composites et des Materiaux Avances, 35 (4) (2025) 643.

[43] Dwech, M., Habeeb, M., and Mohammed, A., Ukrainian Journal of Physics, 67 (10) (2022) 757.

[44] Kadim, A.M., Abass, K.H., Abdali, K., and Musa, S.J., Nano Biomedicine and Engineering, 16 (1) (2024) 119.

[45] Al-Shawabkeh, A.F., Elimat, Z.M., and Abushgair, K.N., J. Thermoplast. Compos. Mater., 36 (2023) 899.

[46] Sharba, K.S., Alkelaby, A.S., Sakhil, M.D., Abass, K.H., Habubi, N.F., and Chiad, S.S., NeuroQuantology, 18 (3) (2020) 66.

[47] Zbala, A.A.K., Al-Ogaili, A.O.M., and Abass, K.H., NeuroQuantology, 20 (2) (2022) 62.

[48] Abass, K.H. and Latif, D.M.A., Int. J. ChemTech Res., 9 (9) (2016) 332.

[49] Wemple, S.H. and DiDomenico, M., Phys. Rev. B, 3 (4) (1971).

[50] Mohemed, B.Y., Alasdi, S., Fakfry, S., Haneen Abass, K., and Mohammed Kadim, A., HORA 2023 - 2023 5th International Congress on Human-Computer Interaction, Optimization and Robotic Applications, Proceedings (2023).